

# Performance and Analysis of a U-Net Model for Automated Skin Lesion Segmentation

Sheetal Nana Patil<sup>1</sup>, Hitendra D. Patil<sup>2</sup>

<sup>1</sup>Research Scholar, Department of Computer Engineering

Shri Shivaji Vidya Prasarak Sanstha's

Bapusaheb Shivajirao Deore College of Engineering, Dhule (MS), India

sheetalpatil2000@gmail.com

<sup>2</sup>Professor, Department of Computer Engineering

Shri Shivaji Vidya Prasarak Sanstha's

Bapusaheb Shivajirao Deore College of Engineering, Dhule (MS), India

hitendradpatil@gmail.com

**Abstract**— A greater proportion of people are affected by skin cancer, particularly melanoma, which has a higher tendency to metastasize. For Dermatologist, Visual inspections are most challenging & complex task for melanoma detection. To solve this problem, dermoscopic images are analyzed and segmented. Due to the sensitivity involved in surgical operations, existing techniques are unable to achieve higher accuracy. As a result, computer-aided systems are essential to detect & segment dermoscopic images.

In this paper, for segmentation 5000 skin images were taken from the HAM10000 dataset. Prior to segmentation, preprocessing is done by resizing images. A novel U Net structure is a fully convolutional network is presented & implemented using up-sampling and down-sampling technique with Rectified Linear Units (ReLU) for activation functions. The outcomes of proposed methodology shows performance improvement for skin-lesion segmentation with 94.7 % pixel accuracy & 89.2 % dice coefficient compared with existing KNN & SVM techniques.

**Keywords**- Accuracy, Dice Coefficient, ReLU; Segmentation, Skin Lesion; U Net.

## I. INTRODUCTION

Melanoma is globally increasing skin disease. In 2022, nearly 3 million new cases found & which is major important public health issue. Visual inspection of the skin surface makes it simple to identify. Unfortunately, most melanomas are missed by clinicians. Professional dermatologists use visual examination to diagnose 60% of cases.

This implies that many potentially curable melanomas go undiscovered until they are extremely advanced. The detection and location of visual dermoscopic skin attributes, as well as the classification of skin-based illnesses, are all dependent on the correct and timely segmentation of skin lesions. Dermoscopy is an imaging technique used to enhance melanoma diagnosis and reduces melanoma mortality, enables deeper layers to be seen visually by reducing skin's surface reflection.



Figure 1. Skin Lesions in Dermoscopic images.

Skin lesions in dermoscopic Images are shown in Figure 1.

It is more challenging to identify and diagnose skin lesions when they are compared to one another in color skin imaging, such as nevus and melanoma. A robust automated method for identifying skin lesions is required since early diagnosis will help to reduce diagnosis time. Early lesion detection will progress cure rate up to 90 %.

Many skin disorder has high similarity appearance, which become more difficult to investigate & causes inaccurate investigation. The lesion should be identified as soon as feasible since, when compared to individuals who have recently

undergone treatment, its survival rate is relatively high. Visual assessment used in Dermoscopic image analysis was unable to identify lesion type assessment.

In this study, we implemented deep learning based U net network and major aspects are as follows.

- To extract the affected region in a skin cancer image, a U net segmentation approach has been developed.
- It is binary segmentation task having an encoder that captures the spatial features and a decoder that up samples the feature maps to produce a segmentation mask.
- For Training Adam optimizer is implemented with binary cross entropy loss function.
- U Net segmentation quantitative measurement is measured with the help of performance parameters.

For skin lesion segmentation, various deep learning based techniques are implemented. These methods irregularly compute the uncertainties of the model and data in their outputs. To put it another way, relying solely on the results of traditional DL and ML algorithms results feature loss during processing & segmentation. In dermoscopic images, melanoma can be automatically found using a variety of techniques. For these methods to be more effective, the lesion site must be isolated.

## II. LITERATURE SURVEY

The significance of early identification and precise diagnosis of melanoma cannot be emphasized. The death rate is rising because to melanoma or other skin conditions. Numerous researchers have expressed interest in improving the diagnosis of these extremely severe skin diseases using different techniques for segmenting skin diseases, including clustering, region expanding, splitting, and supervised and unsupervised learning methods. The literature review examined several influential articles to understand the methodologies and tools employed in previous research, identify gaps, and address limitations.

Skin lesion segmentation is a critical process that involves dividing a single image into smaller parts [1, 2]. Scholars have put forth various methodologies, encompassing both deep learning techniques [3, 4] and traditional segmentation methods [5], to tackle this aspect of skin lesion analysis. Researchers have introduced a hybrid segmentation framework that combines a unique k-means segmentation method [6]. The researchers have defined a two-phase segmentation process. The image is segmented using k-means clustering in the first step to locate the precise lesion region. To obtain higher accuracy, the segmentation is enhanced further in the second phase using the firefly method [7].

In segmentation, two processes are performed. First, histogram-based grouping is employed with the Genetic algorithm. In second stage image pixel set is calculated using the c-means clustering & skin lesion region wise segmentation [8]. Region based segmentation technique is implemented, which works on fuzzy based clustering. In this approach, adjacent pixels are merged based on their spatial context to achieve region growing and segmentation [9]. During image segmentation, similarity index of image is determined by important features like color & texture. In K-means clustering and histogram calculation, segmentation is done by extracting color features [10]. The system described adopts a partially supervised method using the shift mean algorithm to segment skin images. Notably, this method does not necessitate specifying the number of clusters beforehand [11].

Threshold based segmentation technique, in which with reference of threshold value image is divided in multiple regions. This process helps to enhance the clarity of the edges in the cancerous area, aiding in segmentation process [12]. By using skin lesion segmentation method for dermoscopic input images was developed, which combined adaptive thresholding with color network normalization [13]. Numerous researchers designed auxiliary function based technique which creates an auxiliary function which was smoothed using Bezier curves and built using a local minimizer, solving the issue of global optimization [14]. The major objective is to segment low-contrast pixel data using active contour fusion segmentation [15]. For the purpose of identifying the boundary of the skin lesion, a baseline contour without an edge chan-ve is recommended [16].

An exponential neighborhood grey wolf optimization approach was used to optimize a fully convolved network for the segmentation of dermoscopic data [17]. For segmenting the lesion, researcher adapted novel CNN-based architecture [18]. A system that uses Retina- DeepLab, graphical methods and recurrent CNN to segment skin lesions [19]. ResNet and DenseNet in tandem allows for enhancement in a dense encoder-decoder-based system. Furthermore, ASPP used to obtain contextual data and skip connections for image pixel data recovery [20]. The initial feature of the proposed lesion segmentation employing an adaptive twin attention component is an integration of dual modeling approaches using ADAM.

Both multiscale fusion feature & spatial characteristics of image is used to reduce image lost data during segmentation [21]. In convolutional network like iFCN, segmentation of skin lesion without any processing. To minimize the adverse effect of segmentation, lesion location states details around its edge [22]. In [23], a contemporary method is suggested that creates texture and colorful components, which are crucial for evaluating skin cancer. An automated melanoma detection technique using

dermoscopic Images is suggested in [24]. Here, a Gaussian radial basis kernel and an SVM classifier are employed to categories the images [25] introduces an effective machine learning method to melanoma early identification. However, these methods are unable to guarantee superior classification and high-quality segmented images.

In [26], 6 types of algorithm performance was evaluated; in which these algorithms primarily based on thresholding , region , contours, level sets and adaptive thresholding; the algorithm of adaptive snake was implemented to obtain optimum results [27,28], where Delaunay Triangulation was used to divide the image into areas and segment the lesion based on data.

### III. DESIGN & IMPLEMENTATION OF U NET SEGMENTATION

#### A. U-Net Overview & Architecture

Figure 2 shows, semantic segmentation based U-Net architecture contains contracting and expansive path. The contracting route which is analogous to convolutional network.

Each Contracting path is a combination of:

- Two 3x3 unpadding convolutions + Rectified linear unit (ReLU)
- Stride 2 down sampling, Max pooling operation with 2X2.
- Feature channel counts doubled after each down sampling.

Each expansive path is combination of:

- Up Sampling of feature map is an initial stage
- Up-convolution of size 2X2.
- After each up convolution feature channels are reduced by 2.
- Proportionally cropped feature map connected to contracting path
- A number of 2 convolution block of size 3X3.
- ReLU after each convolution block.
- Cropping is essential to regain boundary pixel loss which occurred during convolution.
- In last 1x1 convolution layer is engaged to transfer each 64 feature vector for applicable number of classes.
- The network includes 23 convolutional layers in total.

UNET is a U-shaped encoder-decoder network made up of 4 encoder- decoder sections connected by a bridge. In Each encoder section, feature channels upscale by 2 & spatial dimensions downscaled by 2. Similarly in decoder section spatial dimensions upscale by 2 & feature channels are downscaled by 2.

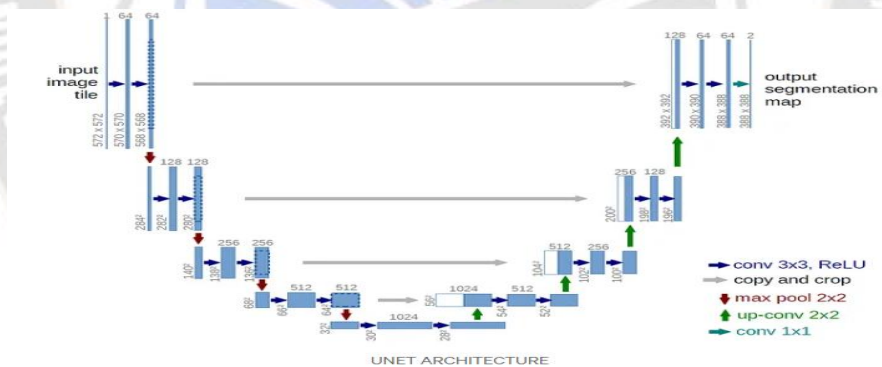


Figure 2. Basic U Net Architecture.

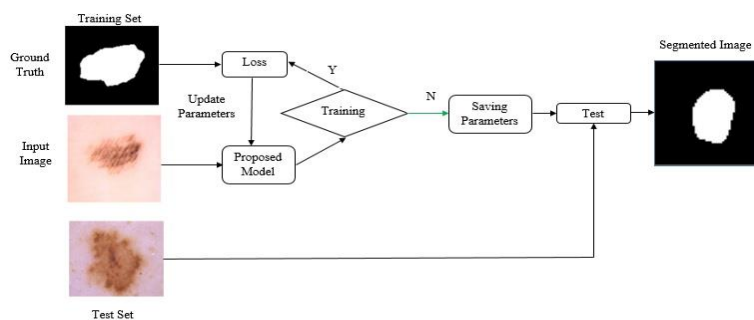


Figure 3. Block Diagram of Proposed U Net skin image segmentation.

TABLE I. DESIGN SPECIFICATION OF PROPOSED U NET SEGMENTATION

Process Block	Block Description	Specification
Input Layer	<ul style="list-style-type: none"> <li>The model initiates input layer, which specifies the incoming data form.</li> </ul>	<ul style="list-style-type: none"> <li>Input shape is (128, 128, 3), indicating that the model expects images with '128' and '128' pixels and 3 color channels (RGB).</li> </ul>
Encoder [3X3]	<ul style="list-style-type: none"> <li>Conv2D layer+ Activation function [ReLU].</li> <li>MaxPooling2D layer which down samples the spatial dimensions by 2.</li> </ul>	<ul style="list-style-type: none"> <li>Conv2D layer + 64 filters</li> <li>Each encoder has Kernel Size 3X3</li> <li>2 D-MaxPooling with (2, 2) size</li> </ul>
Encoder [3X3]	<ul style="list-style-type: none"> <li>Max pooling to preserve the most important features.</li> </ul>	<ul style="list-style-type: none"> <li>Conv2D layer + 128 filters</li> <li>2 D-MaxPooling with (2, 2) size</li> </ul>
Encoder [3X3]	<ul style="list-style-type: none"> <li>Padding ensures the output &amp; input size</li> </ul>	<ul style="list-style-type: none"> <li>Conv2D layer + 256 filters</li> <li>2 D-MaxPooling with (2, 2) size</li> </ul>
<ul style="list-style-type: none"> <li>At this point, the model has performed three stages of encoding, resulting in spatial down sampling and number of filters are increased to capture complex features.</li> </ul>		
Decoder [3X3]	<ul style="list-style-type: none"> <li>Conv2D layer+ Activation function [ReLU].</li> <li>Up sampling for spatial dimensions, features recovery.</li> </ul>	<ul style="list-style-type: none"> <li>Conv2D layer + 512 filters</li> <li>Kernel Size 3X3</li> <li>UpSampling2D layer with a size of (2, 2)</li> </ul>
Decoder [3X3]	<ul style="list-style-type: none"> <li>Concatenation: III<sup>rd</sup> stage encoder output (conv3) is concatenated with preceding output of decoder (up1).</li> <li>Concatenation supports to combine the low &amp; high level features for improved image reconstruction.</li> </ul>	<ul style="list-style-type: none"> <li>Conv2D layer + 256 filters</li> <li>Kernel Size 3X3</li> <li>UpSampling2D layer with a size of (2, 2)</li> </ul>
Decoder [3X3]	<ul style="list-style-type: none"> <li>Concatenation: II<sup>nd</sup> stage encoder output (conv2) is concatenated with preceding output of decoder (up2).</li> </ul>	<ul style="list-style-type: none"> <li>Conv2D layer + 128 filters</li> <li>Kernel Size 3X3</li> <li>UpSampling2D layer with a size of (2, 2)</li> </ul>
Output Layer [1X1]	<ul style="list-style-type: none"> <li>Concatenation: I<sup>st</sup> stage encoder output (conv1) is concatenated with preceding output of decoder (up3).</li> </ul>	<ul style="list-style-type: none"> <li>Conv2D layer + 1 filter</li> <li>Final output produced by Conv2D layer is a binary segmentation mask</li> <li>Segmentation mask represents the regions of interest in the input image.</li> </ul>
Model optimizer & Compilation	<ul style="list-style-type: none"> <li>Adaptive learning Rate optimizer is used</li> <li>Model is assembled using "adam" optimizer</li> <li>With the help of training, "Accuracy" is key performance parameter to access model.</li> </ul>	<ul style="list-style-type: none"> <li>Loss function used is "binary_crossentropy," which is suitable for binary classification tasks.</li> </ul>

*Encoder Network:* By using sequence of encoder blocks, features are extracted from input image [29]. Each encoder block consists of:

- Two 3x3 convolutions separated by a ReLU activation function.
- Non linearity of training data generation is maintained by ReLU activation function.
- ReLU output works like skip connection for applicable decoder block.
- Max Pooling with 2X2: Spatial dimensions feature map is reduced by 2 (height and width).

- Computational time is linear to number of trainable parameters.

*Skip Connections:* Skip connections sends additional data to decoder, to extract precise semantic features. Skip connections act as shortcut path, in which gradient are permitted to connect to older layers without deterioration. During back propagation skip connections improve gradient flow for permitting network to acquire best representation.

*Bridge:* For completing information flow with help of encoders-decoders bridge is essential. Bridge has two sections of 3x3 convolutions separated by a ReLU activation function.

**Decoder Network:** By using abstract representation, the decoder generates a semantic segmentation mask. Encoder block with skip connection feature map is concatenated to 2x2 transpose convolution in the decoder block. Skip connections maintains pixel levels which is lost in network path and depth. In this section, two 3x3 convolutions followed by a ReLU activation function is used.

Final decoder output is directed to 1x1 convolution with sigmoid. The sigmoid activation function helps to create the pixel wise classification in segmentation mask.

#### B. Designing of U Net Model

U Net is a fully convolutional neural network intended to learn less amount of training data. Figure 3 illustrates a Proposed Block diagram of U net segmentation. Initially encoder receives the input Image and then extracts relevant characteristics from it using many convolutional layers.

The features are then up sampled by the decoder using transpose convolution and concatenated using a procedure known as skip connection which results the output in segmentation mask.

Skip connections utilization is another significant element of the U net. As the name implies, a skip link skips part of the neural network layers. The output of one layer is connected to input of following levels. This procedure transfers the chosen features straight from the encoder- network's decoder, allowing decoder to build better segmentation mask.

#### C. U Net Design Parameters

U net segmentation model has several design parameters, Following Table 1 describes Block description & specification used in proposed U Net skin image segmentation

#### D. Model Summary

Following Table 2 shows Layer wise U Net Model Design Summary. The presented model comprises seven convolutional layers.

These convolutional layers extract features and learn hierarchical representations from input Image. U net convolutional layers are elaborated as follows:

Encoder:

- Conv2D layer with 64 filters.
- Conv2D layer with 64 filters.
- Conv2D layer with 128 filters.
- Conv2D layer with 128 filters.

- Conv2D layer with 256 filters.

- Conv2D layer with 256 filters.

Decoder:

- Conv2D layer with 512 filters.

- Conv2D layer with 512 filters.

- Conv2D layer with 256 filters.

- Conv2D layer with 256 filters.

- Conv2D layer with 128 filters.

- Conv2D layer with 128 filters.

Output:

- Conv2D layer with 1 filter.

It's worth noting that, while there are 13 levels in total, some of them are repeated for the encoding and decoding steps. This is a popular design in U-Net-like models, in which the encoder and decoder stages have mirrored topologies, allowing for efficient information transfer between resolution levels. A common application of CNNs involves transforming an image into a vector, often employed for tasks related to classification. In U-Net, initially image is transformed into a vector and vector to image using the identical mapping. In this process distortion is eliminated by keeping the image's original structure.

## IV. RESULTS

### A. Performance Parameters of Segmentation Model:

Performance parameters for image segmentation tasks are crucial in evaluating the quality of the model's predictions. Following are some common performance metrics for segmentation:

- **Intersection-Over-Union (IoU):** IoU evaluates overlapping between the ground truth & predicted masks. It is defined as the union of the masks divided by their intersection.

Dice coefficient = 0 [No overlap],

Dice coefficient = 1 [Complete overlap],

$$IoU = \frac{True\ Positive}{(True\ Positive + False\ positive + False\ Negative)} \quad (4.1)$$

- **Mean Dice coefficient:** The mean Dice coefficient computes the Dice coefficient that is averaged over all samples in the dataset. It returns a single result that represents the model's overall segmentation performance.

TABLE II. LAYER WISE U NET MODEL DESIGN SUMMARY

Layer/Operation	Input Shape	Output Shape	Parameters
input_1	(None, 128, 128, 3)	----	0
conv2d	(None, 128, 128, 64)	(None, 128, 128, 64)	1792
conv2d_1	(None, 128, 128, 64)	(None, 128, 128, 64)	36928
max_pooling2d	(None, 128, 128, 64)	(None, 64, 64, 64)	0
conv2d_2	(None, 64, 64, 64)	(None, 64, 64, 128)	73856
conv2d_3	(None, 64, 64, 128)	(None, 64, 64, 128)	147584
max_pooling2d_1	(None, 64, 64, 128)	(None, 32, 32, 128)	0
conv2d_4	(None, 32, 32, 128)	(None, 32, 32, 256)	295168
conv2d_5	(None, 32, 32, 256)	(None, 32, 32, 256)	590080
max_pooling2d_2	(None, 32, 32, 256)	(None, 16, 16, 256)	0
conv2d_6	(None, 16, 16, 256)	(None, 16, 16, 512)	1180160
conv2d_7	(None, 16, 16, 512)	(None, 16, 16, 512)	2359808
up_sampling2d	(None, 16, 16, 512)	(None, 32, 32, 512)	0
concatenate	(None, 32, 32, 256)	(None, 32, 32, 768)	0
conv2d_8	(None, 32, 32, 768)	(None, 32, 32, 256)	1769728
conv2d_9	(None, 32, 32, 256)	(None, 32, 32, 256)	590080
up_sampling2d_1	(None, 32, 32, 256)	(None, 64, 64, 256)	0
concatenate_1	(None, 64, 64, 128)	(None, 64, 64, 384)	0
conv2d_10	(None, 64, 64, 384)	(None, 64, 64, 128)	442496
conv2d_11	(None, 64, 64, 128)	(None, 64, 64, 128)	147584
up_sampling2d_2	(None, 64, 64, 128)	(None, 128, 128, 128)	0
concatenate_2	(None, 128, 128, 128)	(None, 128, 128, 192)	0
conv2d_12	(None, 128, 128, 192)	(None, 128, 128, 1)	193

TABLE III. U NET PERFORMANCE PARAMETER COMPARISON WITH KNN & SVM SEGMENTATION METHOD.

Performance Parameter	U Net Proposed Method	KNN Existing Method	SVM Existing Method
Mean IoU	0.822	0.778	0.798
Mean Dice Coefficient	0.892	0.675	0.702
Dice Loss	0.108	0.325	0.298
Test Loss	0.141	0.256	0.231
Test accuracy	0.947	0.854	0.875
Precision	0.971	0.890	0.863
Recall	0.923	0.789	0.756

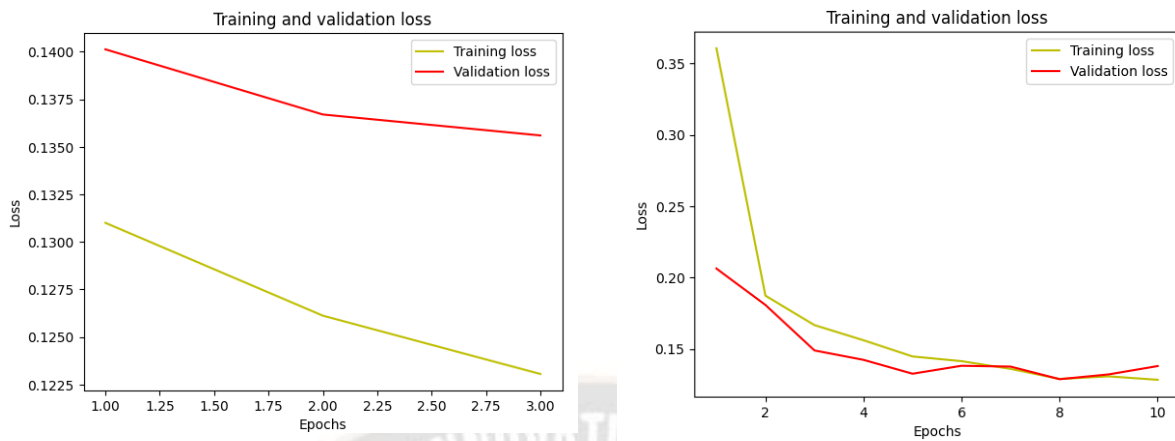
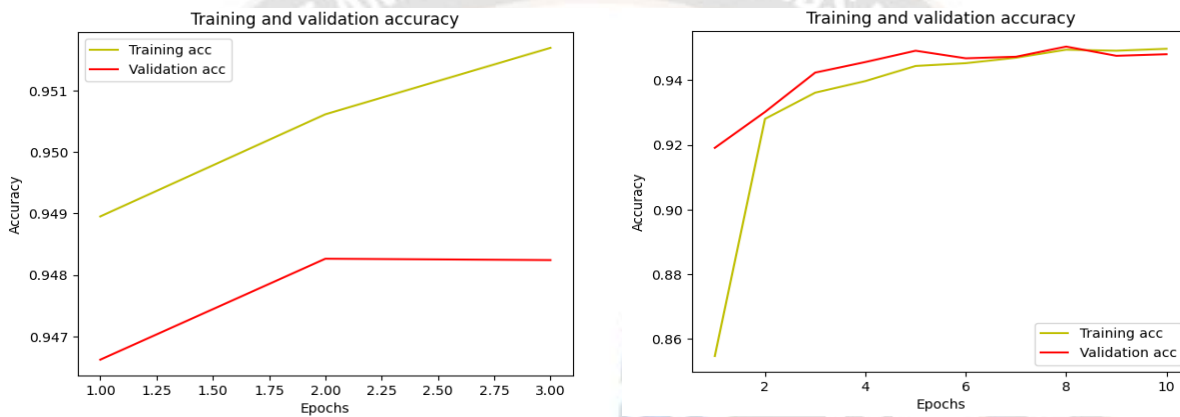


Figure 4. (a) Effect of Epochs on Training & Validation Loss.



(b): Effect of Epochs Training & Validation Accuracy.

The Dice score [29] is utilized for evaluating the resemblance between a predicted segmentation mask and the actual ground truth segmentation mask within the realm of semantic image segmentation. If Dice score is 0 indicate “no overlap” & 1 shows “perfect overlap”.

$$\text{Mean Dice Coefficient} = \frac{2(\text{Area of Overlapped between Predicted \& Ground Truth})}{\text{Total Area of predict and ground truth}} \quad (4.2)$$

Similarly dice coefficient & Dice loss is related to

$$\text{Dice Loss} = 1 - \text{Dice Coefficient} \quad (4.3)$$

- **Test Loss:** Deep learning model prediction is measured by using test loss.

The loss is 0 if the model's forecast is perfect.

The loss is 1 if the model's forecast is inadequate.

- **Test Accuracy:** Accuracy is a metric that characterizes the overall performance of a model across all categories. Test accuracy is useful in all equal classes situation. Test class is a ratio of number of right predictions to the total number of predictions [30].

$$\text{Test Accuracy} = \frac{TP+TN}{TP+FP+TN+FN} \quad (4.4)$$

In equation (4.4),

TP=True Positive

TN=True negative

FP=False positive

FN= False Negative

**Precision:** Precision is calculated by dividing the count of accurately classified positive samples by the total number of positive samples identified, regardless of whether they were classified correctly or incorrectly. Model precision evaluates model accuracy for positive sample classification.

$$\text{Precision} = \frac{TP}{TP+FP} \quad (4.5)$$

**Recall:** Ratio of accurate classified positive sample to the total Positive sample from the population is Recall. The model's recall evaluates its ability to correctly detect positive samples. The recall is proportional to total number of accurate positive sample count.

$$\text{Recall} = \frac{TP}{TP+FN} \quad (4.6)$$

We can obtain insights into how effectively the model performs on the segmentation work by analyzing these performance characteristics and identifying areas for improvement, such as classes with lower IoU or Dice coefficient scores[31]. These indicators are critical for evaluating the segmentation model's efficacy and directing the model's development and fine-tuning [32].

**B. Training, Validation loss & Accuracy**

The training loss is an indicator used to evaluate training data fitment with deep learning model. Training loss calculates the model error on the training data. Training set is an integral part of dataset, which is initially used to train deep learning model. The total of errors for each sample in the training set is used to computationally determine the training loss. Similarly,

validation loss is a parameter which measures deep learning model performance on validation dataset. Validation dataset is used to validate the deep learning model performance.

The validation loss is analogous to training loss, it is a summation of errors occurred from each validation dataset sample.

Above Figure 4 (a) Shows effect of epochs on training & validation loss, it has been observed that after second epoch model effectively working with gradual decrease in training & validation loss (under fitting).

Above Figure 4 (b) Shows epochs count variation on training & validation accuracy, in which second epoch plays vital role to improve training & validation accuracy.

**C. Observational Results on Training Dataset**

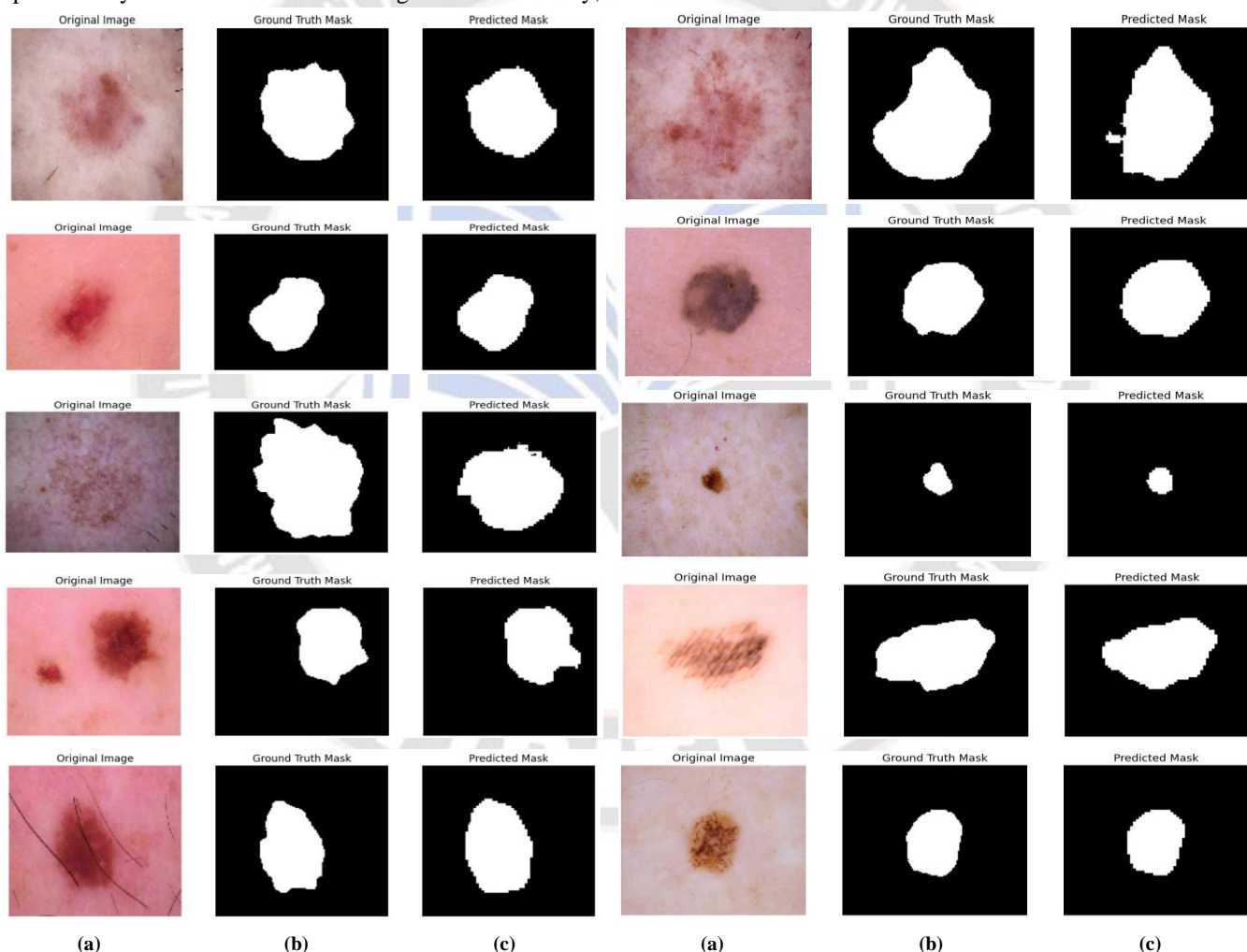


Figure 5. Simulated Results of segmented skin lesion from HAM10000 dataset used for training (a) Original image (b) Ground truth mask; (c) Predicted Mask.

Above Figure 5 Shows (a) Original Image (b) Ground truth mask & (c) Predicted mask using U Net segmentation performed on HAM10000 Training dataset.

D. Observational Results on Testing Dataset

Following Figure 6 Shows (a) Original Image (b) Ground truth mask & (c) Predicted mask using U Net segmentation performed on HAM10000 Testing dataset.

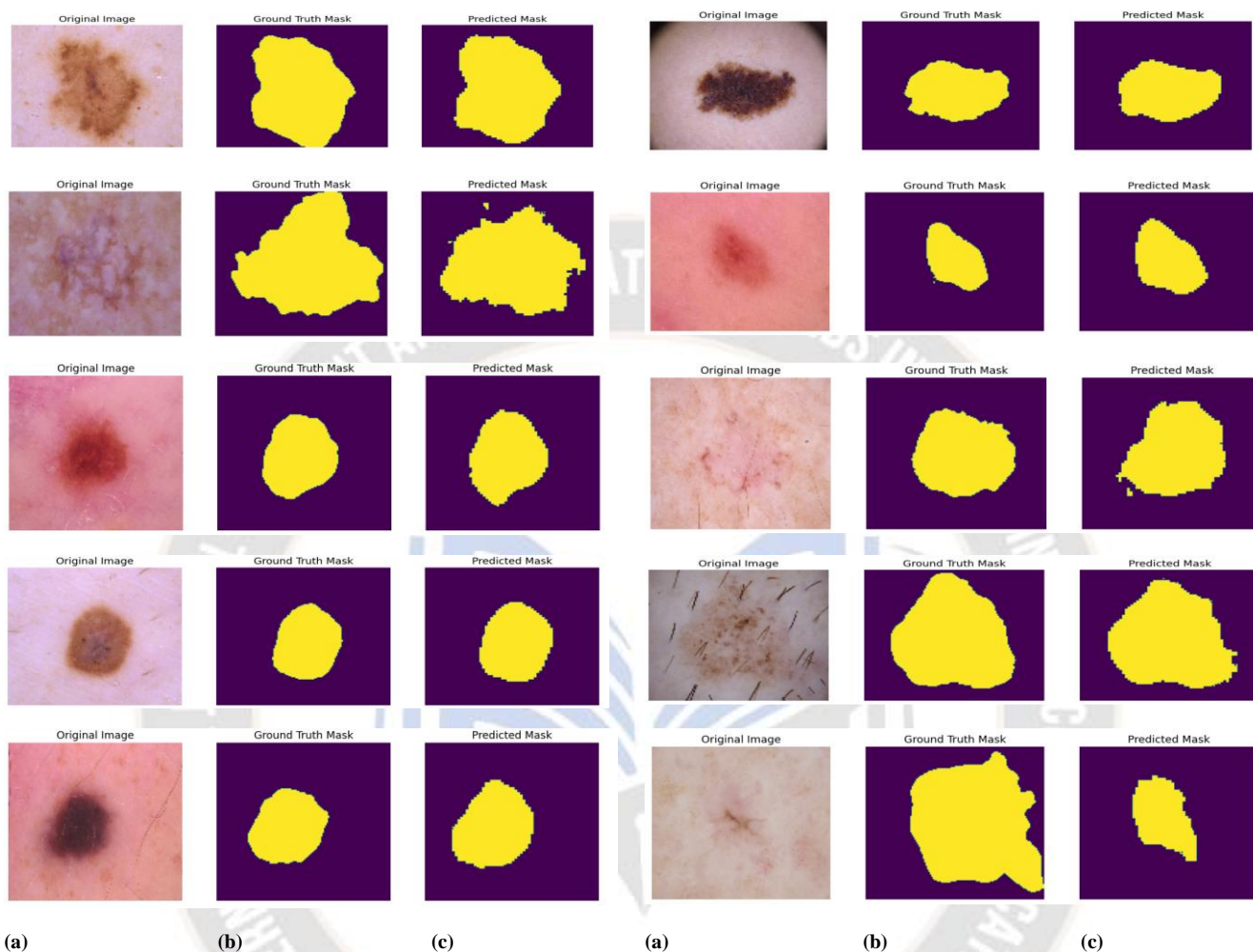


Figure 6. Simulated Results of segmented skin lesion from HAM10000 dataset used for Testing (a) Original image (b) Ground truth mask; (c) Predicted Mask.

V. CONCLUSION & FUTURE WORK

A computerized analysis of skin images can be used by dermatologists to make clinical decisions as well as by patients to evaluate skin lesions outside of the hospital. Initially skin lesions are separated and segmented from the usual skin region, which is primary stage in an automated dermoscopic image analysis. In this research work deep neural network structure is employed for segmenting lesion from skin Images dataset.

An improved jacquard similarity coefficient was achieved as a consequence of segmentation for pre-processed Images. Simulated segmentation results shown improvement in terms of accurate skin lesion region identification, less boundary pixel

loss and better segmented image quality. In future segmented images will be used for binary or multiclass classification purpose, which will be beneficial for dermatologist for diagnosis & treatment.

The proposed test data accuracy is 94.7 % and the loss rate is 14.10 % as a consequence of the segmentation was conducted on HAM 10000 dataset. It is expected that the system's performance would improve if the dataset is expanded, class labels are increased, and other classification and segmentation methods are used. Proposed U-Net segmentation shows exceptional segmentation performance, with the help of characteristics from low-level and high-level layers.

REFERENCES

[1] Iqbal, A.; Sharif, M.; Yasmin, M.; Raza, M.; Aftab, S, "Generative adversarial networks and its applications in the

- biomedical image segmentation: A comprehensive survey”, *Int. J. Multimed. Inf. Retr.*, pp. 333–368, Nov 2022
- [2] Masood, S.; Sharif, M.; Masood, A.; Yasmin, M., “Raza, M. A Survey on Medical Image Segmentation”, *Curr. Med. Imaging*, pp. 3-14, Nov 2015
- [3] Anjum, M.A.; Amin, J.; Sharif, M.; Khan, H.U.; Malik, M.S.A.; Kadry, S., “Deep Semantic Segmentation and Multi-Class Skin Lesion Classification Based on Convolutional Neural Network”, *IEEE Access*, pp. 129668–129678, Aug 2020
- [4] Sayel M. Fayyad, Mohammad Abuzalatah, Mohannad Rawashdeh, A. M. Maqableh, Zaid Abulghanam. (2023). Control, Design and Analysis of Delta 3D Printer . *International Journal of Intelligent Systems and Applications in Engineering*, 11(4s), 444–457. Retrieved from <https://ijisae.org/index.php/IJISAE/article/view/2702>
- [5] Iqbal, A., Sharif, M., Khan, M.A. et al, “FF-UNet: a U-Shaped Deep Convolutional Neural Network for Multimodal Biomedical Image Segmentation”, *Cogn Comput* 14, 1287–1302 (2022).
- [6] Shahzad, A.; Sharif, M.; Raza, M.; Hussain, K., “Enhanced watershed image processing segmentation”, *J. Inf. Commun. Technol.* Vol. 2, No. 1, pp.01-09, Spring 2008.
- [7] Na Hwang, Y.; Seo, M.J.; Kim, S.M, “A Segmentation of Melanocytic Skin Lesions in Dermoscopic and Standard Images Using a Hybrid Two-Stage Approach”, *BioMed Res. Int.* 2021, April 2021, 5562801
- [8] Garg, S.; Jindal, B, “Skin lesion segmentation using k-mean and optimized fire fly algorithm”, *Multimed. Tools*, pp.7397–7410, Appl. 2021, 80.
- [9] Hawas, A.R.; Guo, Y.; Du, C.; Polat, K.; Ashour, A.S, “OCE-NGC: A neutrosophic graph cut algorithm using optimized clustering estimation algorithm for dermoscopic skin lesion segmentation”, *Appl. Soft Comput.* 2020, 86, 105931
- [10] Dr. S.A. Sivakumar. (2019). Hybrid Design and RF Planning for 4G networks using Cell Prioritization Scheme. *International Journal of New Practices in Management and Engineering*, 8(02), 08 - 15. <https://doi.org/10.17762/ijnpm.v8i02.76>
- [11] Mohamed, A.A.I.; Ali, M.M.; Nusrat, K.; Rahebi, J.; Sayiner, A.; Kandemirli, F, “Melanoma skin cancer segmentation with image region growing based on fuzzy clustering mean”, *Int. J. Eng. Innov. Res.* 2017, 6, 91C95.
- [12] Jaisakthi, S.M.; Chandrabose, A.; Mirunalini, P, “Automatic skin lesion segmentation using semi-supervised learning technique”, *arXiv* 2017, arXiv:1703.04301.
- [13] Lynn, N.C.; Kyu, Z.M, “Segmentation and Classification of Skin Cancer Melanoma from Skin Lesion Images”, In *Proceedings of the 2017 18th International Conference on Parallel and Distributed Computing, Applications and Technologies (PDCAT)*, Taipei, Taiwan, pp. 117–122, 18–20, December 2017.
- [14] Saravanan, S.; Heshma, B.; Shanofer, A.A.; Vanithamani, R, “Skin cancer detection using dermoscope images”, *Mater. Today*: , pp. 4823–4827, Proc.2020, 33.
- [15] Thanh, D.N.H.; Erkan, U.; Prasath, V.S.; Kumar, V.; Hien, N.N, “A Skin Lesion Segmentation Method for Dermoscopic Images Based on Adaptive Thresholding with Normalization of Color Models”, In *Proceedings of the 2019 6th International Conference on Electrical and Electronics Engineering (ICEEE)*, Istanbul, Turkey, 16–17 April 2019.
- [16] Abdulhamid, I.A.M.; Sahiner, A.; Rahebi, J, “New Auxiliary Function with Properties in Nonsmooth Global Optimization for Melanoma Skin Cancer Segmentation”, *BioMed Res. Int.* 2020, 2020, 5345923
- [17] Javed, R.; Rahim, M.S.M.; Saba, T.; Rashid, M, “Region-based active contour JSEG fusion technique for skin lesion segmentation from dermoscopic images”, pp.1–10, *Biomed. Res.* 2019, 30.
- [18] Ashour, A.S.; Nagieb, R.M.; El-Khobby, H.A.; Elnaby, M.M.A.; Dey, N, “Genetic algorithm-based initial contour optimization for skin lesion border detection”, *Multimed. Tools*, pp. 2583–2597 Appl. 2021, 80.
- [19] Mohakud, R.; Dash, R, “Skin cancer image segmentation utilizing a novel EN-GWO based hyper-parameter optimized FCEDN”, *J. King Saud Univ.-Comput. Inf. Sci*, pp. 9889–9904, 2022, 34.
- [20] Kaur, R.; Gholam, H.; Sinha, R.; Lindén, M, “Automatic lesion segmentation using atrous convolutional deep neural networks in dermoscopic skin cancer images”, *BMC Med. Imaging*, pp.1–13, 2021, 22.
- [21] Bagheri, F.; Tarokh, M.J.; Ziaratban, M, “Skin lesion segmentation from dermoscopic images by using Mask R-CNN, Retina-Deeplab, and graph-based methods”, *Biomed. Signal Process. Control.* 2021, 67, 102533.
- [22] Emma Smith, *Deep Learning for Gesture Recognition and Human-Computer Interaction*, Machine Learning Applications Conference Proceedings, Vol 3 2023.
- [23] Qamar, S.; Ahmad, P.; Shen, L, “Dense Encoder-Decoder-Based Architecture for Skin Lesion Segmentation”, *Cogn. Comput.* pp.583–594, 2021, 13.
- [24] Wu, H.; Pan, J.; Li, Z.; Wen, Z.; Qin, J, “Automated Skin Lesion Segmentation Via an Adaptive Dual Attention Module”, *IEEE Trans. Med. Imaging*, pp.357–370, 2020, 40.
- [25] Öztürk, S.; Özkaya, U, “Skin Lesion Segmentation with Improved Convolutional Neural Network”. *J. Digit. Imaging*, pp.958–970, 2020, 33.
- [26] Nezhadian, F. K. , and Rashidi, S, “ Melanoma skin cancer detection using color and new texture features” 2017 *Artificial Intelligence and Signal Processing Conference (AISIP)*, Shiraz. pp.1–5, 2017.
- [27] Mustafa, S. and Kimura, A, “A SVM-based diagnosis of melanoma using only useful image features”, 2018 *International Workshop on Advanced Image Technology (IWAIT)*, ChiangMai. pp.1–4, 2018.
- [28] Waheed, Z., Waheed, A., Zafar, M. and Riaz, F, “ An efficient machine learning approach for the detection of melanoma using dermoscopic images”, 2017 *International Conference on Communication, Computing and Digital Systems (C-CODE)*, Islamabad. pp.316–319, 2017.
- [29] Silveira, M., Nascimento, J. C., Marques, J. S., Marçal, A. R., Mendonça, T., Yamauchi, S., Maeda, J., and Rozeira, J, “Comparison of segmentation methods for melanoma diagnosis in dermoscopy images”, *IEEE J. Sel. Top. Signal Process* 3(1):pp.35–45, 2009
- [30] Pennisi, A., Bloisi, D.D., Nardi, D., Giampetruzzi, A. R., Mondino, C., and Facchiano, A, “ Skin lesion image segmentation using Delaunay triangulation for melanoma detection” *Comput. Med. Imaging Graph.* 52:89–103, 2016.

- 
- [31] Maglogiannis, I., Doukas, C. N., and Member, S, "Overview of advanced computer vision Systems for Skin Lesions Characterization", IEEE Trans. Inf. Technol. Biomed. 13(September):721–733, 2009.
- [32] Tushar H. Jaware , K. B. Khanchandani , Anita Zurani, "An Accurate Automated Local Similarity Factor-Based Neural Tree Approach toward Tissue Segmentation of Newborn Brain MRI ", Am J Perinatol 2019; 36(11): 1157-1170, DOI: 10.1055/s-0038-1675375
- [33] Jaware, T.H., Patil, V.R., Badgular, R.D. et al. Performance investigations of filtering methods for T1 and T2 weighted infant brain MR images. *Microsyst Technol* 27, 3711–3723 (2021). <https://doi.org/10.1007/s00542-020-05144-6>
- [34] Tushar Jaware, Kamlesh Khanchandani & Ravindra Badgular, "A novel hybrid atlas-free hierarchical graph-based segmentation of newborn brain MRI using wavelet filter banks" *International Journal of Neuroscience*, vol 130 (5), pp 499–514, 2020
- [35] P. G. Patil et al., "Marathi Speech Intelligibility Enhancement Using I-AMS Based Neuro-Fuzzy Classifier Approach for Hearing Aid Users," in *IEEE Access*, vol. 10, pp. 123028-123042, 2022, doi: 10.1109/ACCESS.2022.3223365.

